https://doi.org/10.5194/egusphere-2026-3321
Preprint. Discussion started: 19 June 2026

Divergent responses of streamflow reanalysis errors to precipitation reanalysis errors modulated by catchment heterogeneity

Qiang Li[1], Tongtiegang Zhao[1,*], Zexin Chen[1], Zeqing Huang[2]

[1]Southern Marine Science and Engineering Guangdong Laboratory (Zhuhai), School of Civil Engineering, Sun Yat-Sen University, Guangzhou, China
[2]Department of Civil and Environmental Engineering, The Hong Kong University of Science and Technology, Hong Kong SAR, China.

Correspondence to: Tongtiegang Zhao (zhaottg@mail.sysu.edu.cn)

Abstract. Streamflow reanalysis is vital for water resources management and climate impact assessment; however, the extent to which it is affected by precipitation forcing errors remains poorly understood. Focusing on the reanalysis dataset of Global Flood Awareness System driven by the European Centre for Medium-Range Weather Forecasts Reanalysis v5 (GloFAS-ERA5), this paper details how streamflow reanalysis errors respond to precipitation errors. Specifically, the root mean square errors (RMSEs) are calculated by hydrological year for reanalysis products across 671 catchments in the Catchment Attributes and Meteorology for Large-sample Studies (CAMELS) dataset; and by combining catchment-specific linear regression with global panel regression, the effects of precipitation errors on streamflow errors are quantified. The results demonstrate an improved performance from GloFAS-ERA5 v2.1 to v4.0, with the median RMSE decreasing from 2.16 mm to 1.81 mm. For GloFAS-ERA5 v4.0, the panel regression indicates that for every 1 mm increase in precipitation RMSE, the corresponding streamflow RMSE increases by an average of 0.51 mm–reflecting the buffering capacity of catchment storage. In the meantime, the corresponding catchment-specific increase of streamflow RMSE reaches up to 2.5 mm in humid catchments but remains below 0.7 mm in arid catchments. These divergent responses reflect that the saturation-excess mechanism makes the precipitation errors immediately affect the streamflow error while soil moisture deficits dampen their effects. Furthermore, incorporating interaction terms into panel regression increases the coefficient of determination (R^2) from 0.16 to 0.36, indicating that error responses are modulated by catchment heterogeneity. This modulation is further confirmed by targeted case studies, indicating that the temperature controls the storage and release of snow water, thereby dampening and delaying the responses of streamflow errors to precipitation errors in snow-dominated catchments. These findings provide a valuable diagnostic method and practical guidance for applications of global streamflow reanalysis to complex, heterogeneous catchments.

https://doi.org/10.5194/egusphere-2026-3321
Preprint. Discussion started: 19 June 2026

1 Introduction

Streamflow reanalysis provides valuable spatiotemporally continuous data for water resource management and climate impact assessment (Nourani et al., 2026; Liu et al., 2023; Zhao et al., 2024). To overcome the lack of direct spatiotemporal observations, regional to global datasets of streamflow reanalysis are generated by forcing hydrological models with climate reanalysis (Yang et al., 2021; Grimaldi et al., 2023). One leading global streamflow reanalysis dataset is generated by using the Global Flood Awareness System (GloFAS) under the forcing of the European Centre for Medium-Range Weather Forecasts (ECMWF) Reanalysis v5 (ERA5), known as GloFAS-ERA5 (Harrigan et al., 2020, 2023; Alfieri et al., 2020). Evaluated with daily observations, the GloFAS-ERA5 is shown to be more skillful than the mean flow benchmark in 86% of 1801 catchments worldwide (Harrigan et al., 2020). As a result, it has been widely utilized for investigating large-scale variability (Ficchì and Stephens, 2019), calibrating hydrological models (Senent-Aparicio et al., 2021; Mbuvha et al., 2022), training machine learning algorithms (Rahman et al., 2022) and providing benchmark references (Nearing et al., 2024).

The local performance is a critical issue for global hydrological datasets (Zhu et al., 2023; Harrigan et al., 2020; Nourani et al., 2026). Previous investigations highlighted that the performance of GloFAS-ERA5 varies considerably across catchments (Harrigan et al., 2020; Prudhomme et al., 2024; Zhao et al., 2024). For instance, systematic negative biases are prevalent across Europe, North America and central Southern America while positive biases have been observed in central United States, Africa and western coast of South America (Harrigan et al., 2020). As precipitation is the primary driver of the hydrologic cycle, these performance discrepancies are profoundly influenced by the quality of precipitation reanalysis (Tang et al., 2023; Wang et al., 2023). The inherent nonlinearity of hydrological processes implies that precipitation errors can be either amplified or dampened in streamflow reanalysis (Nanding et al., 2021a; Miao et al., 2024; Meng and Zhao, 2025). The error propagations are furthermore complicated by catchment attributes (Ma et al., 2026; Zhu et al., 2023). For example, high meltwater fractions from snow and glaciers can dampen the responses of streamflow to precipitation in the eastern High Mountain Asia (Zhu et al., 2023).

While the performance of streamflow reanalysis has been evaluated using spatiotemporal verification metrics (Zhao et al., 2024; Chen et al., 2022; Harrigan et al., 2020), the specific responses of streamflow reanalysis errors to precipitation reanalysis errors across different catchments remain poorly understood (Nanding et al., 2021a; Zhang et al., 2026). To this end, this paper is concentrated on how streamflow reanalysis errors respond to precipitation errors. Specifically, the root mean square error (RMSE) values for reanalysis products are calculated by hydrological year across 671 catchments in the Catchment Attributes and Meteorology for Large-sample Studies (CAMELS) dataset; and the effects of precipitation errors on streamflow errors are quantified by combining catchment-specific linear regression with global panel regression, including pooled, random-effects, entity fixed-effects and two-way fixed-effects frameworks. The objectives are 1) to compare the performance of GloFAS-ERA5 v2.1 and v4.0; 2) to quantify the responses of streamflow reanalysis errors to precipitation errors; 3) to analyze the influence of catchment attributes on these error responses; and 4) to illustrate the divergent responses through catchment case studies.

https://doi.org/10.5194/egusphere-2026-3321
Preprint. Discussion started: 19 June 2026

2 Data

2.1 Streamflow reanalysis and observations

The GloFAS-ERA5 provides global gridded daily time series of streamflow reanalysis (Harrigan et al., 2020). There is recently an upgraded from v2.1 to v4.0 (Table 1), resulting from fundamental changes in model architecture with the spatial resolution improving from 0.1° to 0.05° (Prudhomme et al., 2024). In GloFAS-ERA5 v2.1, the OS LISFLOOD hydrological model is primarily utilized for channel routing, forced by surface and sub-surface runoff data from the Hydrology Tiled ECMWF Scheme for Surface Exchanges over Land (HTESSEL) within ERA5 (Zhao et al., 2024). By contrast, the GloFAS-ERA5 v4.0 is forced directly by atmospheric variables from ERA5, enabling the LISFLOOD to internally simulate the entire rainfall-runoff and routing processes (Prudhomme et al., 2024).

Table 1. Streamflow datasets used in the investigation.

Dataset	Variables	Type	Resolution	Coverage	Reference
GloFAS-ERA5 v2.1	Streamflow	Reanalysis	0.1°×0.1°, daily	Global land, 1979-present	(Harrigan et al., 2020)
GloFAS-ERA5 v4.0	Streamflow	Reanalysis	0.05°×0.05°, daily	Global land, 1979-present	(Grimaldi et al., 2023)
CAMELS	Streamflow	Observation	Station, daily	the contiguous USA, 1980-2010	(Addor et al., 2017; Newman et al., 2015)

The streamflow observations corresponding to reanalysis are sourced from the CAMELS dataset (Addor et al., 2017; Newman et al., 2015). This dataset comprises 671 catchments across the contiguous United States, characterized by minimal anthropogenic disturbances and a wide range of hydroclimatic conditions. Streamflow observations from stations and catchment-mean meteorological forcing data from Daymet, Maurer and NLDAS are provided at the daily timescale. This dataset also provides static attributes related to climate, soils, vegetation, topography and geology (Addor et al., 2017). To align the gridded GloFAS-ERA5 reanalysis with station observations, the Kling–Gupta efficiency (KGE) is calculated between observations and the reanalysis data from the nine nearest grid cells. Then the time series from the grid cell with the highest KGE is selected as the corresponding reanalysis data for that station (Zhao et al., 2022).

https://doi.org/10.5194/egusphere-2026-3321
Preprint. Discussion started: 19 June 2026

2.2 Precipitation reanalysis and observations

The climate reanalysis of precipitation, as well as temperature, are sourced from the ERA5 dataset (Table 2) (Hersbach et al., 2020). It integrates global observations with model output based on data assimilation (Ishida et al., 2024). The ERA5 provides spatiotemporally complete and consistent reanalysis data of global climate, including hourly estimates of a wide range of atmospheric, ocean-wave and land-surface variables from January 1940 to present. In the analysis, the daily catchment-mean precipitation and temperature are extracted from the raw ERA5 reanalysis of 0.25°×0.25°.

The observations of precipitation, as well as temperature, are sourced from the Daymet dataset (Thornton et al., 2016). By interpolating and extrapolating ground-based observations, it generates long-term, continuous, gridded estimates of daily meteorological variables over continental North America, Hawaii and Puerto Rico. Due to its high resolution of 1km×1km, the Daymet is widely utilized in hydrological modeling (Frame et al., 2023; Newman et al., 2015). As provided in the CAMELS dataset, the catchment-mean Daymet precipitation and temperature are used in the analysis.

Table 2. Climate datasets used in the investigation.

Dataset	Variables	Type	Resolution	Coverage	Reference
ERA5	Precipitation, temperature	Reanalysis	0.25°×0.25°, hourly	Global, 1940-present	(Hersbach et al., 2020)
Daymet	Precipitation, temperature	Observation	1km×1km, daily	North America, 1980-present	(Thornton et al., 2016)

3 Methods

3.1 Quantification of reanalysis errors

The root mean square error (RMSE) is used to quantify the overall discrepancies between reanalysis products and observations (Huang and Zhao, 2022; Liu and Lei, 2026). For each catchment, the RMSE values of streamflow (eQ_i), precipitation (eP_i) and temperature (eT_i) are calculated as follows:

https://doi.org/10.5194/egusphere-2026-3321
Preprint. Discussion started: 19 June 2026

$$\begin{cases} eQ_i = \sqrt{\frac{1}{K_i}\sum_{k=1}^{K_i}(Q_{i,k} - \hat{Q}_{i,k})^2} \\ eP_i = \sqrt{\frac{1}{K_i}\sum_{k=1}^{K_i}(P_{i,k} - \hat{P}_{i,k})^2} \\ eT_i = \sqrt{\frac{1}{K_i}\sum_{k=1}^{K_i}(T_{i,k} - \hat{T}_{i,k})^2} \end{cases} \quad (1)$$

where $\hat{Q}_{i,k}$, $\hat{P}_{i,k}$ and $\hat{T}_{i,k}$ denote the streamflow, precipitation and temperature reanalysis for catchment i, respectively; $Q_{i,k}$, $P_{i,k}$ and $T_{i,k}$ represent the corresponding observations, respectively; K_i is the total number of data pairs for catchment i.

To capture the temporal variability of reanalysis errors, RMSE values are also calculated by hydrological year spanning from 1 October to the next 30 September (Frame et al., 2023). These annual RMSE values are subsequently used for regression analysis. The annual RMSE values of streamflow ($eQ_{i,t}$), precipitation ($eP_{i,t}$) and temperature ($eT_{i,t}$) are calculated:

$$\begin{cases} eQ_{i,t} = \sqrt{\frac{1}{n_{i,t}}\sum_{d=1}^{n_{i,t}}(Q_{i,t,d} - \hat{Q}_{i,t,d})^2} \\ eP_{i,t} = \sqrt{\frac{1}{n_{i,t}}\sum_{d=1}^{n_{i,t}}(P_{i,t,d} - \hat{P}_{i,t,d})^2} \\ eT_{i,t} = \sqrt{\frac{1}{n_{i,t}}\sum_{d=1}^{n_{i,t}}(T_{i,t,d} - \hat{T}_{i,t,d})^2} \end{cases} \quad (2)$$

where $\hat{Q}_{i,t,d}$, $\hat{P}_{i,t,d}$ and $\hat{T}_{i,t,d}$ respectively denote the streamflow, precipitation and temperature reanalysis for catchment i on day d of hydrological year t; $Q_{i,t,d}$, $P_{i,t,d}$ and $T_{i,t,d}$ represent the corresponding observations, respectively; $n_{i,t}$ is the number of data pairs in hydrological year t for catchment i.

3.2 Linear regression for individual catchment

The linear regression is used to identify the responses of streamflow reanalysis errors to precipitation reanalysis errors (Over et al., 2025; Anderson et al., 2022; Steinschneider et al., 2013). The catchment-specific linear regression avoids the assumptions regarding the homogeneity of the error responses across all catchments that are needed for panel regression models (Over et al., 2025; Anderson et al., 2022). For each catchment, it is fitted using the ordinary least squares estimator:

$$eQ_{i,t} = \beta_1^i eP_{i,t} + \beta_2^i eT_{i,t} + \beta_0^i + \epsilon_{i,t} \quad (3)$$

where β_1^i and β_2^i represent the regression coefficients for precipitation and temperature errors in catchment i, respectively; β_0^i and $\epsilon_{i,t}$ denotes the regression intercept and residuals, respectively. The β_1^i quantifies how much streamflow reanalysis error responds to every 1 mm increase in precipitation reanalysis error. The coefficient of determination (R^2) is used to quantify the

https://doi.org/10.5194/egusphere-2026-3321
Preprint. Discussion started: 19 June 2026

goodness-of-fit for regression models (Wang et al., 2026; Over et al., 2025; Steinschneider et al., 2013). For linear regression of catchment i, the R^2 is calculated:

$$R^2 = 1 - \frac{\sum(eQ_{i,t} - \widehat{eQ}_{i,t})}{\sum(eQ_{i,t} - \overline{eQ}_i)} \quad (4)$$

Where $\widehat{eQ}_{i,t}$ and $\overline{eQ}_i$denote the fitted value and mean value of $eQ_{i,t}$, respectively.

3.3 Panel regression across all catchments

Panel regression can be used to quantify the average response using both the spatial and temporal dimensions of the errors (Steinschneider et al., 2013). The pooled panel regression assumes no heterogeneity across catchments:

$$eQ_{i,t} = \beta_1 eP_{i,t} + \beta_2 eT_{i,t} + \beta_0 + \epsilon_{i,t} \quad (5)$$

where β_1 and β_2 are the average effects of precipitation errors and temperature errors on streamflow errors across all catchments, respectively; β_0 and $\epsilon_{i,t}$ denotes the regression intercept and residuals, respectively. The random-effects panel regression accounts for unobserved time-invariant variations across catchments. It assumes that these individual effects are uncorrelated with the included independent variables:

$$eQ_{i,t} = \beta_1 eP_{i,t} + \beta_2 eT_{i,t} + \beta_0 + \alpha_i + \epsilon_{i,t} \quad (6)$$

where α_i is a random independent variable that represents the individual effects of catchment i. The fixed-effects panel regression assumes that omitted factors controlling the dependent variable are correlated with the included independent variables. The entity fixed-effects model is utilized:

$$eQ_{i,t} = \beta_1 eP_{i,t} + \beta_2 eT_{i,t} + \mu_i + \epsilon_{i,t} \quad (7)$$

where μ_i is the intercept representing individual effect for catchment i that is constant in time and characterizes the time-averaged heterogeneity. The two-way fixed-effects model is used to further consider synchronous region-wide temporal shocks:

$$eQ_{i,t} = \beta_1 eP_{i,t} + \beta_2 eT_{i,t} + \mu_i + \lambda_t + \epsilon_{i,t} \quad (8)$$

where λ_t is the intercept representing the time fixed effect for hydrological year t.

To evaluate how catchment attributes influence the error responses of streamflow reanalysis, the random-effects panel regression is extended by incorporating with interaction terms between climate reanalysis errors and catchment attributes:

$$eQ_{i,t} = \beta_1 eP_{i,t} + \beta_2 eT_{i,t} + \beta_3 PS_i eP_{i,t} + \beta_4 SF_i eT_{i,t} + \beta_0 + \alpha_i + \epsilon_{i,t} \quad (9)$$

where PS_i and SF_i respectively represent the seasonality and timing of precipitation (hereafter precipitation seasonality) and the fraction of precipitation falling as snow (hereafter snow fraction) for catchment i that are included in the CAMELS dataset. The marginal effects of the precipitation reanalysis error (β_1') and temperature reanalysis error (β_2') are the first derivative of Eq. (9) with respect to the corresponding independent variables:

https://doi.org/10.5194/egusphere-2026-3321
Preprint. Discussion started: 19 June 2026

$$\begin{cases} \beta_1' = \beta_1 + \beta_3 PS_i \\ \beta_2' = \beta_2 + \beta_4 SF_i \end{cases} \quad (10)$$

where β_3 and β_4 are the regression coefficients of the two interaction terms, respectively. They capture how catchment attributes linearly modulate the baseline average effects of precipitation error and temperature error (β_1 and β_2).

3.4 Experimental design

Experiment 1. Verification of reanalysis data

Using the observations from the CAMELS dataset, the performance of GloFAS-ERA5 v2.1 and v4.0 streamflow reanalysis is verified and then compared by the RMSE metric. The ERA5 precipitation and temperature reanalysis are verified against the Daymet observations. Furthermore, based on the RMSE values by hydrological year, the Pearson's correlation coefficients (r) between streamflow, precipitation and temperature errors are calculated both within individual catchments and across all catchments to assess their underlying collinearity .

Experiment 2. Responses of streamflow errors to precipitation errors

To investigate how streamflow reanalysis errors respond to precipitation errors, the linear regression is fitted for each single catchment. Meanwhile, four panel regression models, i.e., the pooled, random-effects, entity fixed-effects and two-way fixed-effects frameworks, are utilized to quantify the average responses across all catchments. The spatial heterogeneity of error responses is identified by comparing catchment-specific linear regression with the global panel regression.

Experiment 3. Influence of catchment heterogeneity

To analyze how catchment heterogeneity modulates the error responses, the relationships between catchment-specific linear regression coefficients and static catchment attributes are investigated. Furthermore, by incorporating interaction terms into the random-effects panel regression, this analysis isolates and quantifies the marginal effects of precipitation and temperature errors, revealing how catchment heterogeneity diversify the error responses.

Experiment 4. Catchment-specific divergent error responses

Based on the statistical findings in Experiment 3, the in-depth case studies of two selected catchments are conducted to validate the divergent responses of streamflow reanalysis errors. By analyzing specific hydrological processes in rain-dominated versus snow-dominated catchments, the case studies offer physical insights into why streamflow reanalysis errors exhibit divergent responses to precipitation reanalysis errors across different catchments.

https://doi.org/10.5194/egusphere-2026-3321
Preprint. Discussion started: 19 June 2026

4 Results

4.1 Verification of reanalysis data

The statistical and spatial distributions of reanalysis errors quantified by RMSE are shown in Fig. 1. As the GloFAS-ERA5 is upgraded from v2.1 to v4.0, the median RMSE across 671 catchments decreases from 2.16 mm to 1.81 mm. Due to the improvement of performance, the subsequent analyses focus on the GloFAS-ERA5 v4.0. Spatially, both streamflow and precipitation reanalysis errors are influenced by regional aridity. The higher RMSE values are predominantly found in the humid Eastern and Western coastal regions, while lower errors are observed in the arid Midwest region. The correlation coefficient between streamflow and precipitation reanalysis errors increases from 0.27 for GloFAS-ERA5 v2.1 to 0.45 for v4.0, highlighting the critical role of precipitation accuracy in streamflow reanalysis. By contrast, temperature reanalysis errors peak primarily in the complex topography of the western mountainous region. The overall correlation between streamflow and temperature reanalysis errors remains near zero for both GloFAS-ERA5 versions, suggesting that temperature errors do not exert a consistent direct influence on streamflow errors across all catchments.

https://doi.org/10.5194/egusphere-2026-3321
Preprint. Discussion started: 19 June 2026

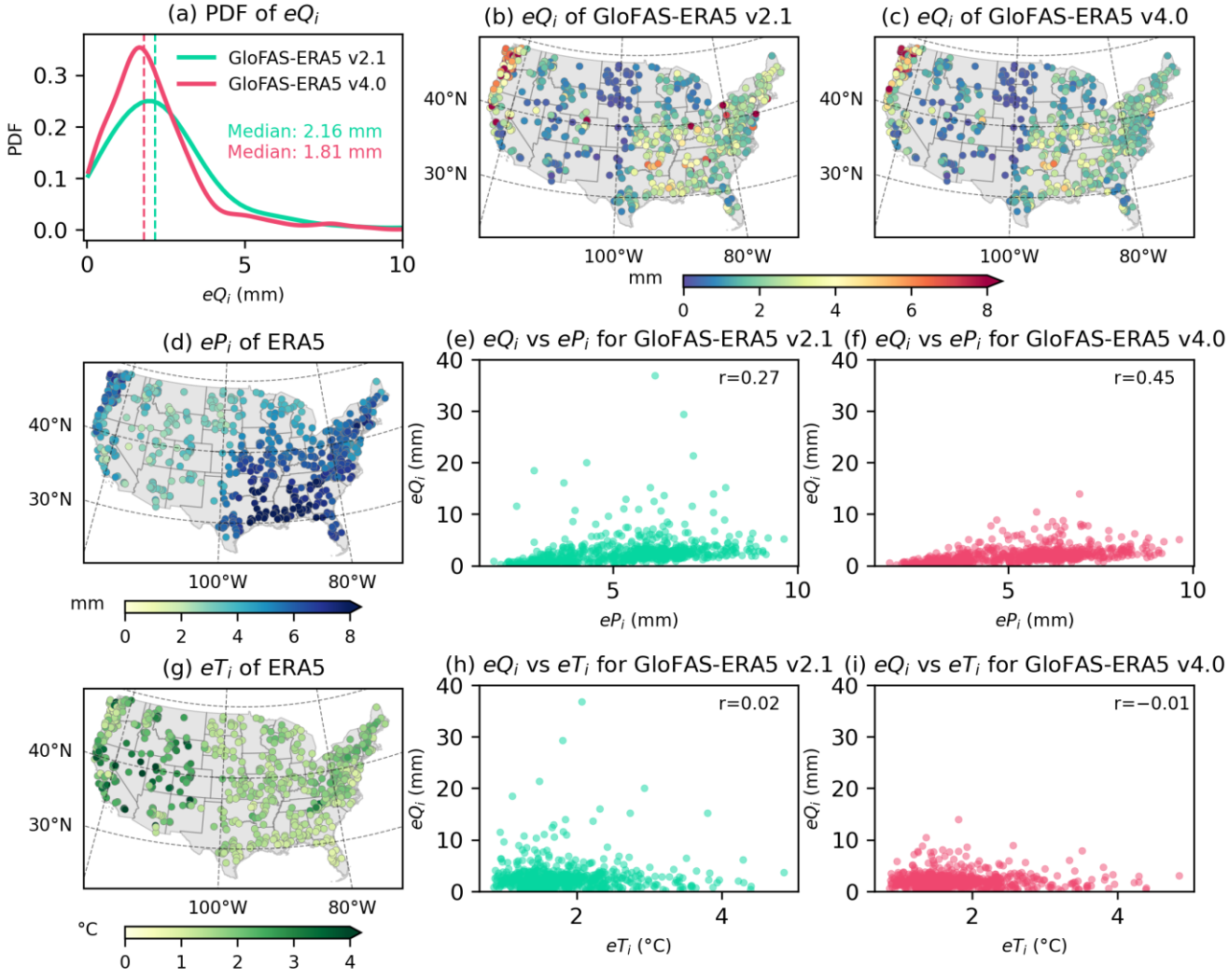

Figure 1. Statistical and spatial distributions of reanalysis errors. (a-c) Probability distribution function (PDF) and spatial distribution of streamflow reanalysis errors for GloFAS-ERA5 v2.1 and v4.0. (d-i) Spatial distribution of precipitation reanalysis errors and temperature reanalysis errors, as well as their relationships with streamflow reanalysis errors.

The relationships among annual RMSE of streamflow, precipitation and temperature reanalysis are illustrated in Fig. 2. Significant positive correlations between streamflow and precipitation errors are observed in 567 (85% of 671) catchments. The coefficients for individual catchments range from 0 to 0.88 with the median value of 0.56, while the correlation for pooled data across all catchments is 0.44. By contrast, the correlation between streamflow and temperature errors is unstable and statistically insignificant in 603 (90% of 671) catchments. The local coefficients fluctuate widely between −0.68 and 0.65 with the median value of −0.04, while the correlation for pooled data across all catchments is −0.01. In addition, the correlation between precipitation and temperature errors is insignificant in 535 (80% of 671) catchments, with the median value of 0.13

https://doi.org/10.5194/egusphere-2026-3321
Preprint. Discussion started: 19 June 2026

195 compared to −0.22 for pooled data. Their Variance Inflation Factor (VIF) values are consistently below 5 across all catchments, indicating that collinearity between precipitation and temperature errors is negligible. Consequently, both variables can be utilized as independent predictors in the subsequent regression models.

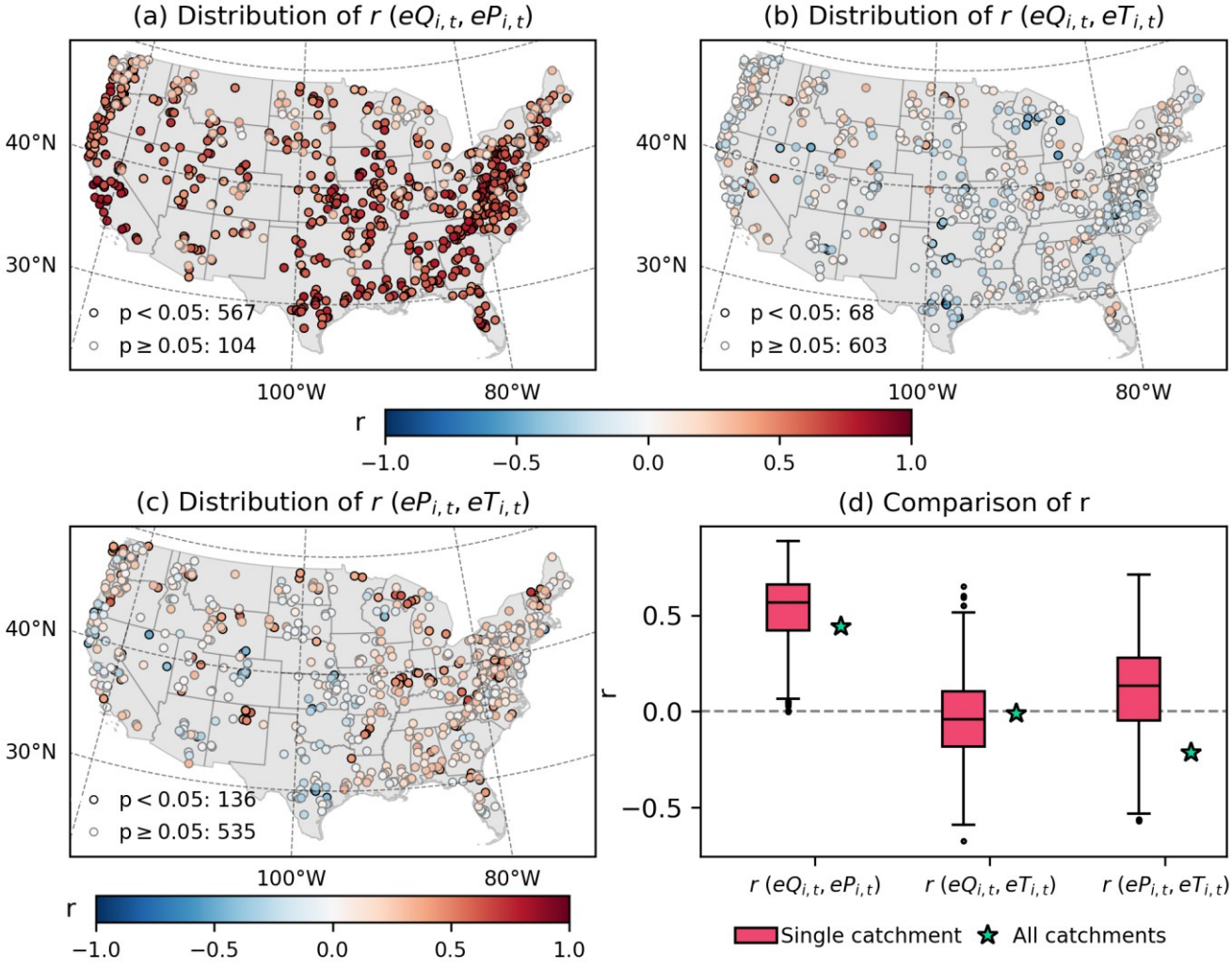

200 **Figure 2.** Pearson's correlation coefficients (r) of reanalysis errors by hydrological year. (a-c) Spatial distribution of r among streamflow, precipitation and temperature reanalysis errors, as well as (d) comparison between r across single catchments (boxplots) and r of all pooled catchments (star markers). Boxes represent the interquartile range (IQR) and the median value across single catchments. Whiskers extend to the data points within 1.5 times the IQR from the box.

https://doi.org/10.5194/egusphere-2026-3321
Preprint. Discussion started: 19 June 2026

4.2 Responses of streamflow errors to precipitation errors

The streamflow reanalysis errors and their corresponding estimations from panel regression models are shown in Fig. 3. While the R^2 ranges from 0.15 to 0.20, the p-values of all regression coefficients are below 0.01, indicating that precipitation and temperature reanalysis errors significantly affect the streamflow reanalysis errors. Except for the pooled panel regression, the regression coefficients of the other three panel regression models are close. The p-value of the Breusch-Pagan Lagrange multiplier test is less than 0.01, confirming the presence of heteroscedasticity. Since the pooled panel regression cannot account for the unobserved heterogeneity across catchments, it is inadequate for capturing the average effects here (Steinschneider et al., 2013). Although the Hausman test suggests a marginal statistical preference for the entity fixed-effects model with p-value of 0.03, the results of the two-way fixed-effects model do not differ significantly from the random-effects model. Consequently, the random-effects panel regression is selected for subsequent analyses due to its computational efficiency. The coefficient of precipitation error for the random-effects panel regression is 0.52, indicating that for every 1 mm increase in precipitation RMSE, the corresponding streamflow RMSE increases by an average of 0.51 mm.

https://doi.org/10.5194/egusphere-2026-3321
Preprint. Discussion started: 19 June 2026

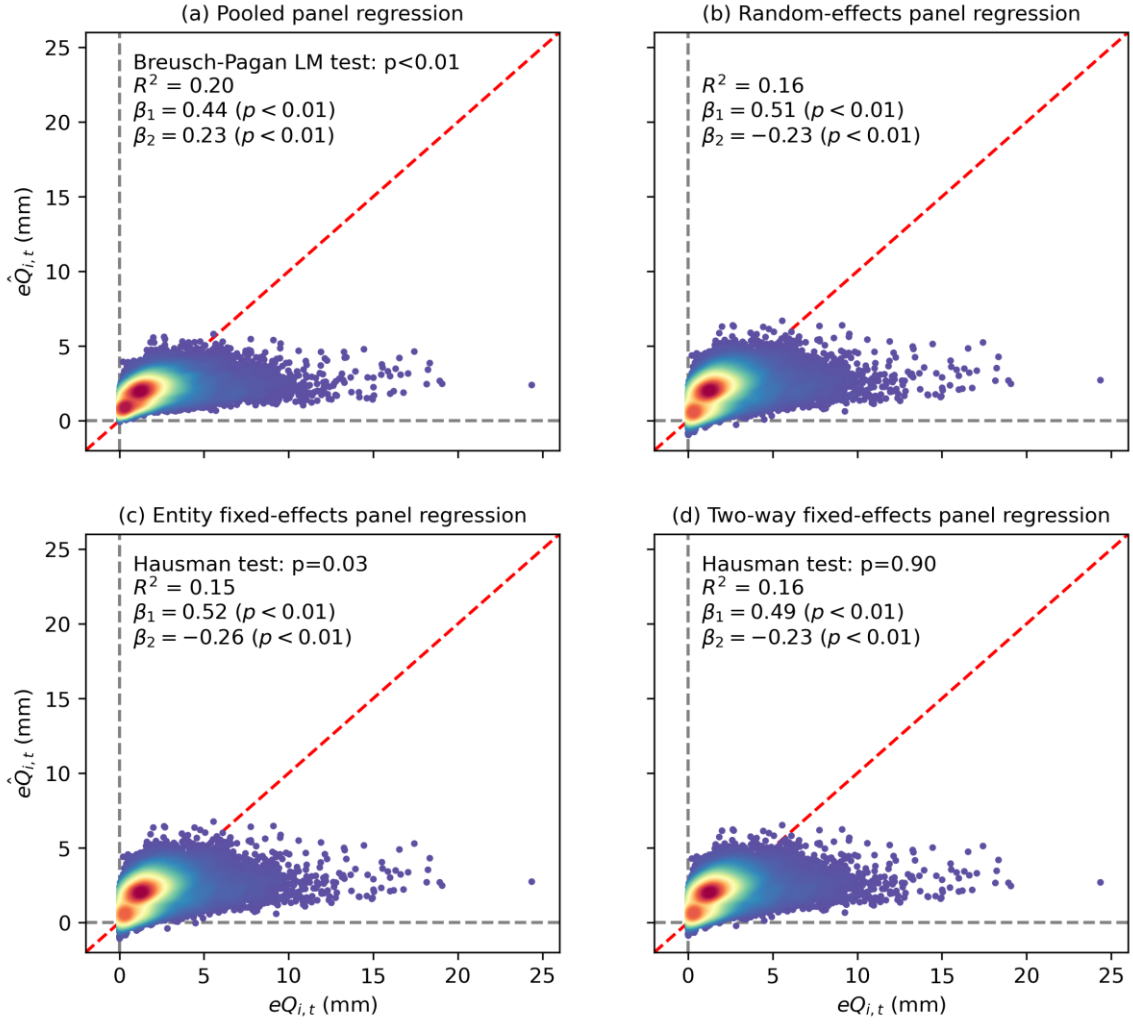

Figure 3. Streamflow reanalysis errors and the estimated errors for (a) pooled, (b) random-effects, (c) entity fixed-effects and (d) two-way fixed-effects panel regression.

The local responses of streamflow reanalysis errors for individual catchments are compared with the average responses across all catchments, as shown in Fig. 4. Compared with the Southeastern U.S. and the West Coast, the R^2 is lower in the central and the western mountainous regions, likely due to the high nonlinearity of runoff processes in these arid and complex terrains. The median R^2 of linear regression across the 671 catchments is 0.36, outperforming the random-effects panel regression's R^2 of 0.16. Similar to R^2, the local effects of precipitation reanalysis errors are positive and statistically significant in 564 (84% of 671) catchments, where the corresponding regression coefficients are relatively high (from nearly 0 to 2.5) in humid catchments (aridity index < 2) but low (from nearly 0 to 0.7) in arid catchments (aridity index ≥ 2). The aridity index is calculated as the ratio of mean potential evapotranspiration to mean precipitation. The panel regression

https://doi.org/10.5194/egusphere-2026-3321
Preprint. Discussion started: 19 June 2026

230 coefficients roughly correspond with the central distribution of catchment-specific linear regression coefficients. Across the 671 catchments, the median coefficients of precipitation errors and temperature errors are respectively 0.43 and −0.17, while the coefficients are respectively 0.51 and −0.23 for the panel regression. While the panel regression provides a stable estimate of the average error responses across all catchments, it inherently masks the divergent local responses (Anderson et al., 2022).

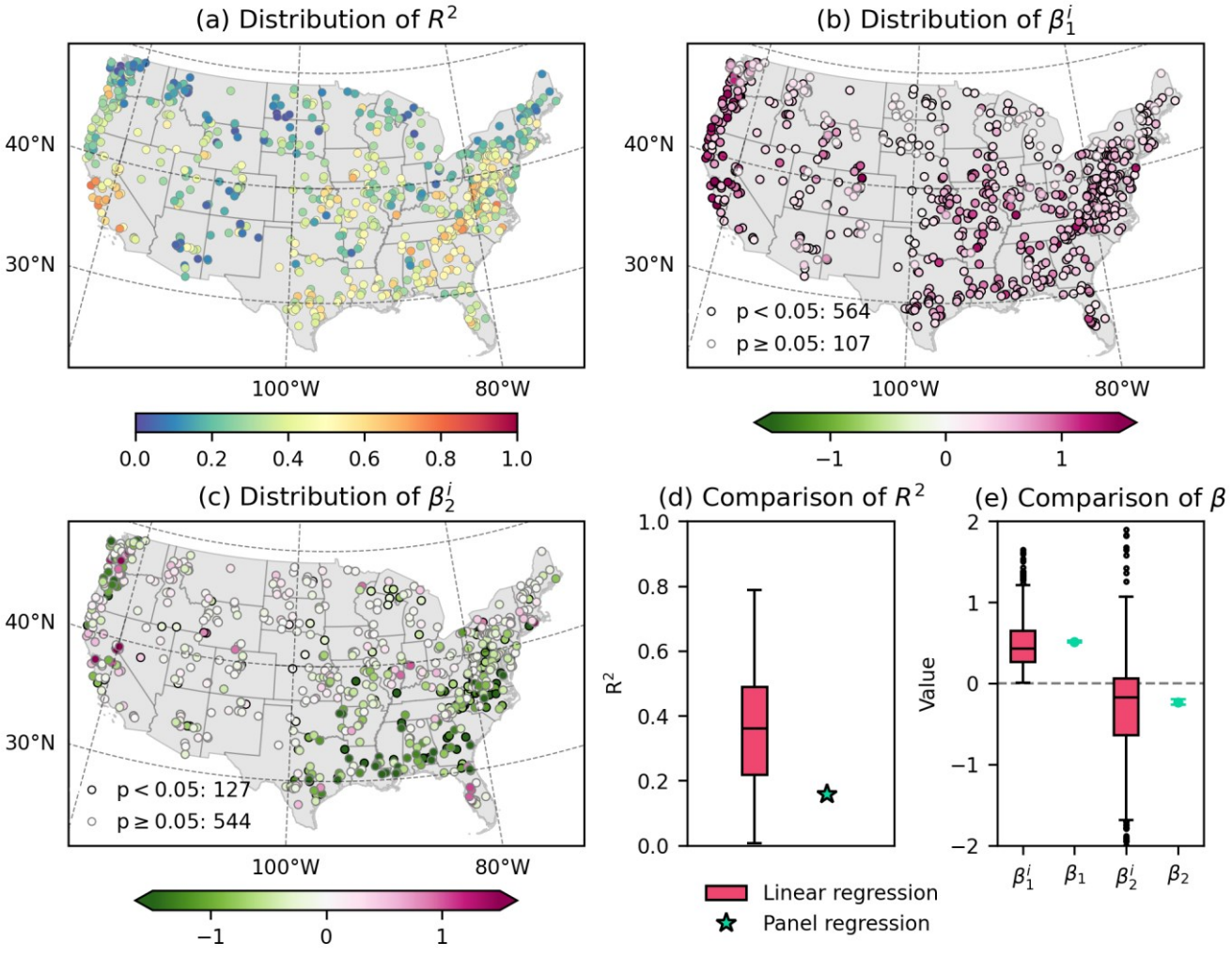

235

Figure 4. Responses of streamflow reanalysis errors quantified by catchment-specific linear regression and global panel regression. (a) Coefficient of determination, (b) effects of precipitation reanalysis errors and (c) effects of temperature reanalysis errors for linear regression, as well as (d, e) their comparison with those of random-effects panel regression. Box and whisker descriptions are as in Fig. 2.

https://doi.org/10.5194/egusphere-2026-3321
Preprint. Discussion started: 19 June 2026

4.3 Influence of catchment heterogeneity

The relationships between local error responses quantified by linear regression and catchment attributes are shown in Fig. 5. The R^2 is negatively correlated with the latitude and the snow fraction, with the correlation coefficients of −0.43 and −0.29, respectively. This result suggests that the linear regression tends to capture more error variance in warmer, lower-latitude catchments than in snow-dominated regions. The effects of precipitation reanalysis errors are negatively correlated with precipitation seasonality and aridity index but positively related with mean precipitation. The correlation coefficients are respectively −0.36, −0.25 and 0.31. This result suggests that the the saturation-excess mechanism makes the precipitation errors immediately affect the streamflow error in humid catchments while soil moisture deficits dampen their effects in arid catchments. In the meantime, the effects of temperature reanalysis errors are positively correlated with latitude, snow fraction and elevation. It indicates that temperature errors become the important drivers of streamflow reanalysis errors in high-latitude or mountainous catchments where snowmelt processes are critical. These correlations indicate that the responses of streamflow errors are influenced by the specific physical and climatic characteristics of the catchments.

https://doi.org/10.5194/egusphere-2026-3321
Preprint. Discussion started: 19 June 2026

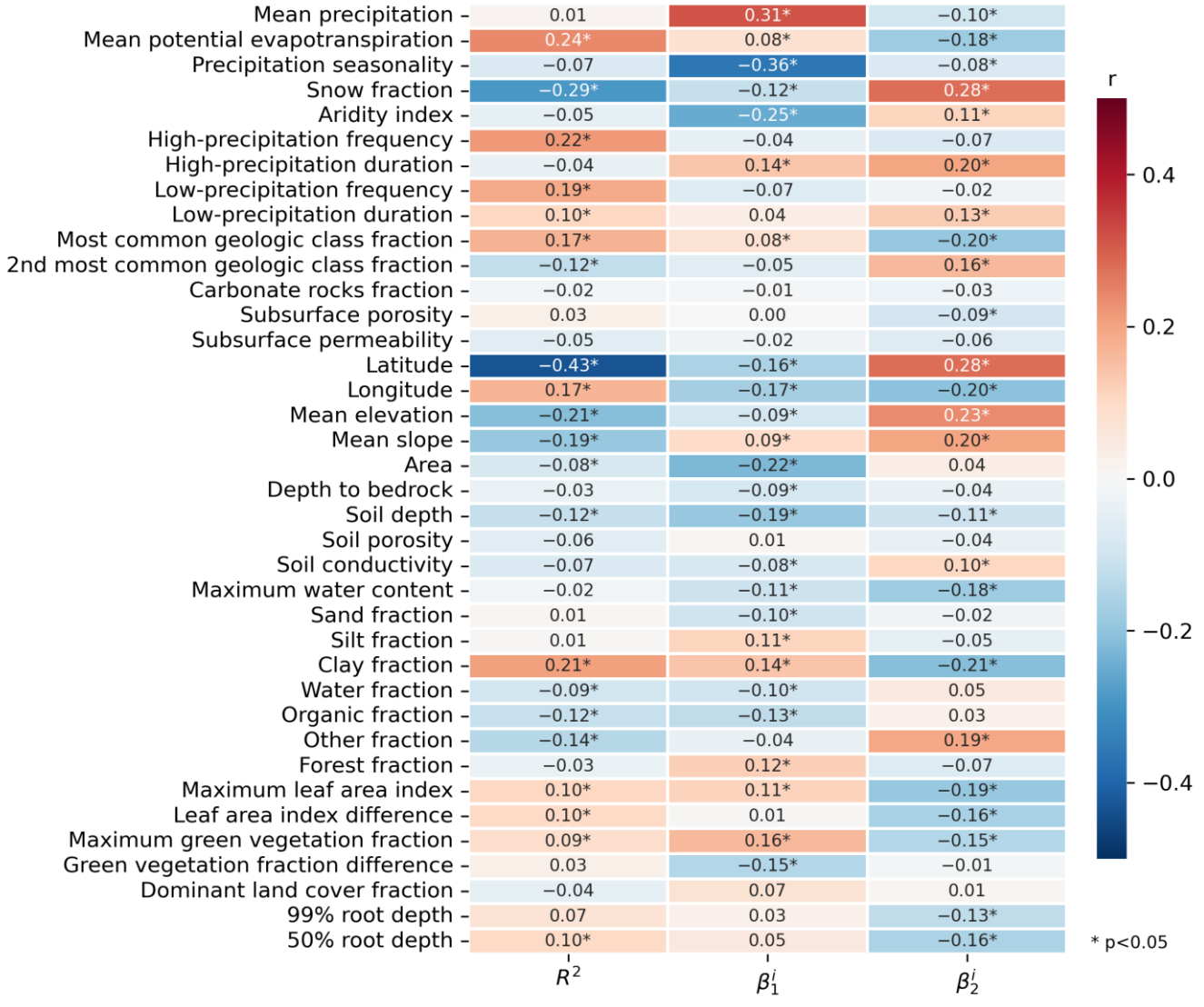

Figure 5. Pearson's correlation coefficients (r) between catchment attributes in the CAMELS dataset and the coefficient of determination(R^2), effects of precipitation reanalysis errors ($\boldsymbol{\beta_1^i}$) and effects of temperature errors ($\boldsymbol{\beta_2^i}$) for catchment-specific linear regression.

The modulating influences of precipitation seasonality and snow fraction on the effects of precipitation and temperature reanalysis errors are illustrated in Fig. 6. For catchments with statistically significant linear regression coefficients, the effects of precipitation reanalysis errors are negatively correlated with precipitation seasonality. The correlation coefficient is −0.38. The effects of temperature reanalysis errors are positively related with snow fraction, with the correlation coefficient of 0.52. By incorporating these hydroclimatic attributes into the panel regression via two interaction terms as specified in Eq. (9), the model's explanatory power improves substantially, with the R^2 increasing from 0.16 to 0.36. The derived marginal

https://doi.org/10.5194/egusphere-2026-3321
Preprint. Discussion started: 19 June 2026

effects reveal a systematic shift in error propagation. Specifically, as the value of precipitation seasonality increases, the precipitation regimes transition from winter-concentrated to summer-concentrated patterns and the marginal effects of precipitation errors decrease. In the meantime, the marginal effects of temperature errors amplify as the snow fraction increases, indicating that the effects of temperature errors are enhanced in snow-dominated catchments. These trends are consistent with the local responses derived from catchment-specific linear regression.

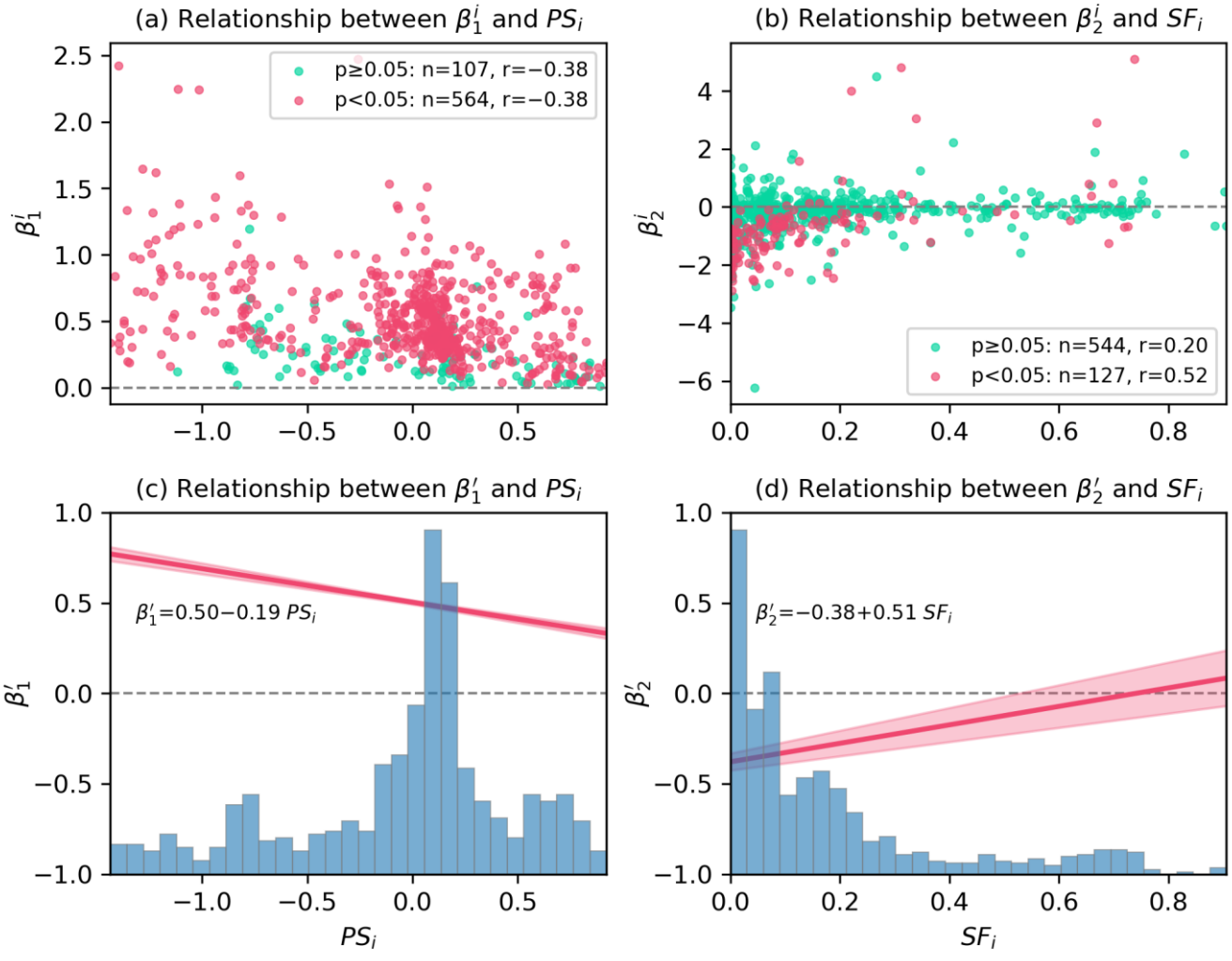

Figure 6. Relationships between effects of reanalysis errors and hydroclimatic attributes of catchments. Scatter plots illustrate the relationship between (a) effects of precipitation errors and precipitation seasonality and (b) effects of temperature errors and snow fraction. Panels (c) and (d) show the marginal effects of precipitation reanalysis errors as a function of precipitation seasonality and temperature reanalysis errors as a function of snow fraction, respectively. In (a) and (b), r and n respectively denote the Pearson's correlation coefficient and the number of catchments where the linear regression coefficients are statistically significant ($p<0.05$) or insignificant ($p\geq0.05$). In (c) and (d), the solid red lines represent the marginal effects derived from the random-effects panel regression with interaction terms in Eq. (10) with shaded 95% confidence intervals. The histograms show the distributions of respective catchment attributes.

https://doi.org/10.5194/egusphere-2026-3321
Preprint. Discussion started: 19 June 2026

4.4 Catchment-specific divergent error responses

The reanalysis data and observations of precipitation, temperature and streamflow for the rain-dominated catchment 14166500 are showcased in Fig. 7. The responses of streamflow reanalysis errors are almost synchronous with the precipitation errors. Specifically, the periods where GloFAS-ERA5 underestimates streamflow peaks are consistent with instances where ERA5 underestimates precipitation. The effect of precipitation errors is statistically significant with the regression coefficients of 0.69, indicating that the streamflow errors increase with precipitation errors. By contrast, the effect of temperature errors is statistically insignificant, demonstrating that temperature fluctuations play a negligible role in the error responses of this rain-dominant catchment. Among hydrological years spanning from 2009 to 2011, the highest precipitation error occurred in 2011 with the RMSE of 5.15 mm, leading to the largest streamflow RMSE of 1.41 mm. This case study indicates that in humid rain-dominated catchments, the performance of streamflow reanalysis is almost entirely dependent on the accuracy of precipitation reanalysis rather than temperature.

https://doi.org/10.5194/egusphere-2026-3321
Preprint. Discussion started: 19 June 2026

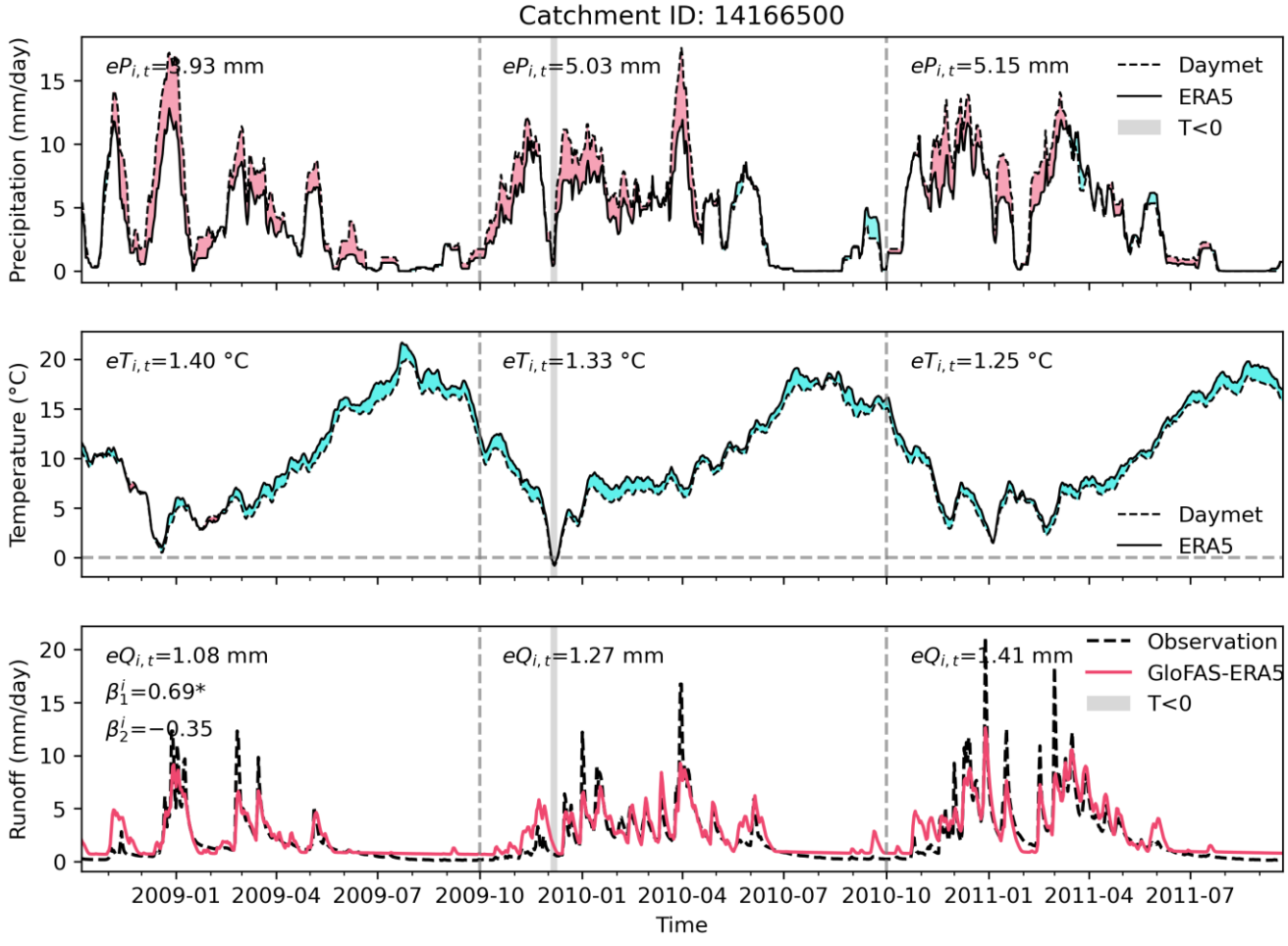

Figure 7. Reanalysis data and observations of precipitation, temperature and streamflow for the rain-dominated catchment 14166500. The asterisk denotes regression coefficient that is statistically significant ($p<0.05$).

The reanalysis data and observations of precipitation, temperature and streamflow for the snow-dominated catchment 13310700 are showcased in Fig. 8. This catchment is characterized by substantial snow accumulation from November to next March, followed by a seasonal surge in runoff starting in April as the rising temperature triggers snowmelt. The streamflow errors are driven jointly by precipitation and temperature errors. Both effects are statistically significant with regression coefficients of 0.43 and 0.37, respectively. Among hydrological years spanning from 1998 to 2000, the precipitation error and streamflow error in 1999 are simultaneously the highest with the RMSE of 3.81 mm and 1.37 mm, respectively. Although the precipitation error in 1998 equals to that in 2000, the streamflow error in 1998 is higher due to the larger temperature error. The underestimation of precipitation from November to next March leads to the deficit in simulated snow storage, while the underestimation of temperature from April to June delays and reduces simulated snowmelt. Consequently, these combined

https://doi.org/10.5194/egusphere-2026-3321
Preprint. Discussion started: 19 June 2026

errors result in the underestimation of GloFAS-ERA5 streamflow from April to June. These results confirm that in snow-dominated catchments, temperature reanalysis errors directly interfere with the simulated timing and magnitude of snowmelt, thereby amplifying streamflow reanalysis errors.

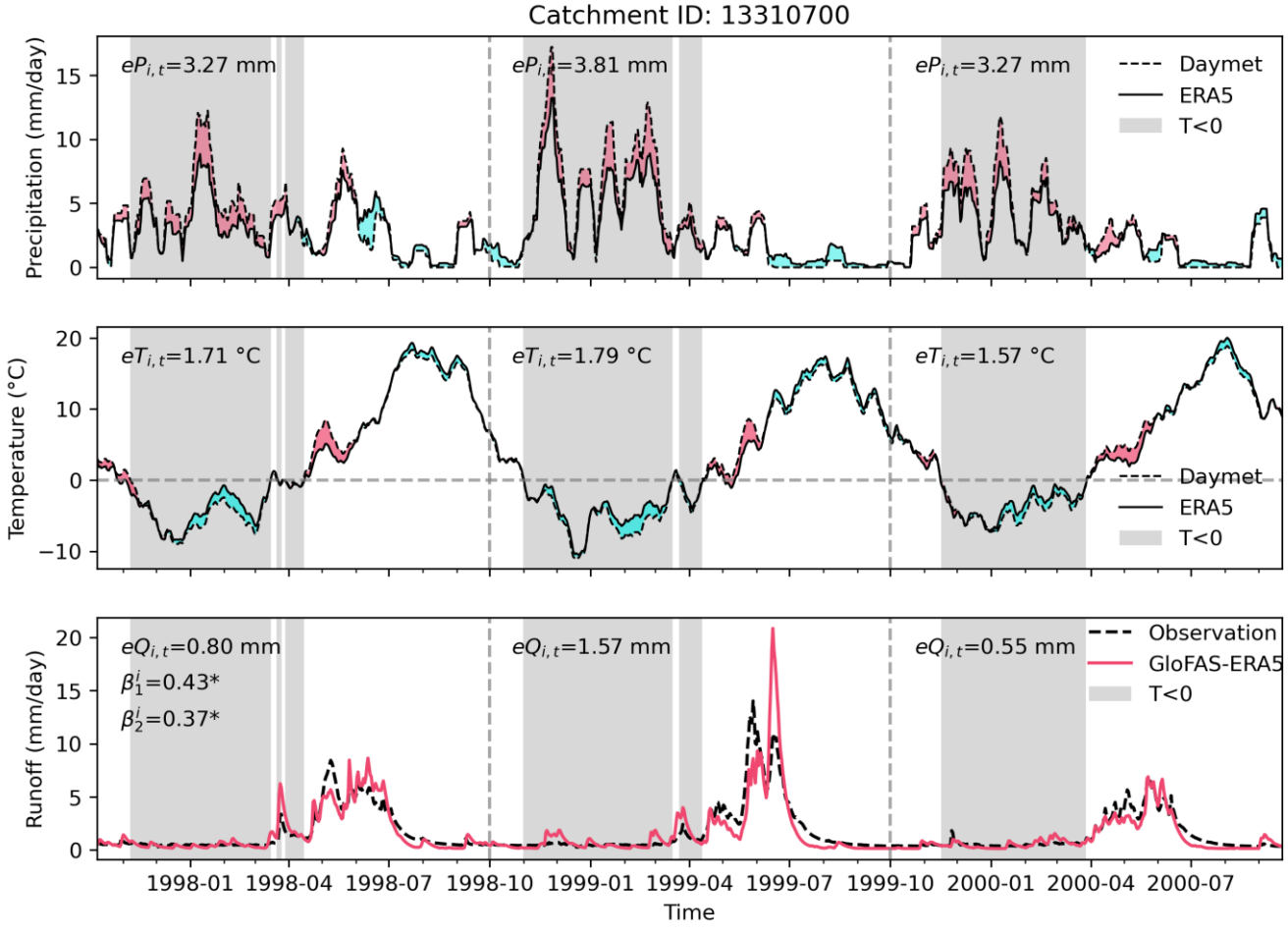

Figure 8. As for Fig. 7, but for the snow-dominated catchment 13310700.

5 Discussion

The performance of streamflow reanalysis is primarily constrained by climate forcings, initial conditions, representation of physical processes and model parameterization (Liu et al., 2023; Nourani et al., 2026; Nanding et al., 2021b). Due to the improvements of hydrological model and calibration method, the performance of GloFAS-ERA5 enhances when

https://doi.org/10.5194/egusphere-2026-3321
Preprint. Discussion started: 19 June 2026

upgraded from v2.1 to v4.0 (Prudhomme et al., 2024; Alfieri et al., 2020). Since the precipitation uncertainty is generally identified as the primary driver to the errors in the simulated streamflow (Tang et al., 2023; Wang et al., 2023), this paper quantifies the responses of streamflow reanalysis errors to precipitation reanalysis errors through catchment-specific linear regression and global panel regression. The panel regression shows that precipitation reanalysis errors have a statistically significant average effect on streamflow reanalysis errors. This result aligns with previous findings of the positive linear relationships between precipitation and streamflow errors (Nanding et al., 2021a; Wu et al., 2017). In the meantime, the panel regression coefficients roughly correspond with the central distribution of linear regression coefficients, indicating the reliability of panel regression in capturing average effects from large-sample datasets (Anderson et al., 2022; Over et al., 2025).

Due to inherent catchment heterogeneity, each catchment has unique and often unmeasured characteristics that may affect hydrological processes (Anderson et al., 2022; Zhu et al., 2023; Ma et al., 2026). While the linear regression is effective for uncovering local relationships within individual catchments, it often lacks the generalizability required to characterize hydrological responses across larger number of catchments (Anderson et al., 2022; Steinschneider et al., 2013). By contrast, the standard panel regression assumes that the responses of streamflow reanalysis errors to precipitation errors are homogeneous across all catchments, thereby ignoring the influence of catchment heterogeneity (Over et al., 2025; Anderson et al., 2025). This paper incorporates two interaction terms into the panel regression to account for the influence of precipitation seasonality and snow fraction. These two moderators effectively account for the fact the responses of streamflow errors to climate forcing errors depends on the specific catchment conditions (Nanding et al., 2021a; Miao et al., 2024). For instance, in high-latitude or mountainous regions, the seasonal storage and delayed release of snowmelt can weaken the streamflow responses to immediate precipitation events (Zhu et al., 2023; Wang et al., 2021; McMillan, 2020). These findings reflect that catchment heterogeneity modulates the responses of streamflow errors to precipitation errors.

6 Conclusions

This paper has investigated the divergent responses of streamflow reanalysis errors to precipitation reanalysis errors. Specifically, the RMSE values of GloFAS-ERA5 streamflow reanalysis, ERA5 precipitation and temperature are calculated by hydrological year across 671 catchments in the CAMELS dataset; and the catchment-specific linear regression and global panel regression are combined to quantify the error responses of streamflow reanalysis. The results show that as the GloFAS-ERA5 is upgraded from v2.1 to v4.0, the performance of streamflow reanalysis improves, with the median RMSE across 671 catchments decreasing from 2.16 mm to 1.81 mm. For GloFAS-ERA5 v4.0, the panel regression analysis indicates that the average effect increases the streamflow RMSE by 0.51 mm in response to every 1 mm increase in precipitation RMSE. For catchment-specific linear regression, the corresponding increase of streamflow RMSE is relatively high in humid catchments (up to 2.5 mm) but low in arid catchments (below 0.7 mm). The divergent responses reflect that the saturation-excess mechanism makes the precipitation errors immediately affect the streamflow error in humid catchments while soil moisture

https://doi.org/10.5194/egusphere-2026-3321
Preprint. Discussion started: 19 June 2026

deficits dampen their effects in arid catchments. Furthermore, incorporating interaction terms into the panel regression increases the coefficient of determination from 0.16 to 0.36, indicating that marginal effects of precipitation errors are modulated by catchment heterogeneity. This modulation is further confirmed by case studies of the rain-dominated and snow-dominated catchments. Overall, these findings provide a useful diagnostic method and practical guidance for applications of global streamflow reanalysis to heterogeneous catchments.

Code and data availability

The GloFAS-ERA5 streamflow reanalysis v2.1 and v4.0 can be downloaded from the CEMS Early Warning Data Store at https://ewds.climate.copernicus.eu/datasets/cems-glofas-historical (Harrigan et al., 2020). The CAMELS dataset can be sourced from the US National Center for Atmospheric Research at https://ral.ucar.edu/solutions/products/camels (Addor et al., 2017; Newman et al., 2015). The Daymet is also provided in the CAMELS dataset. The ERA5 can be downloaded from the Copernicus Climate Data Store at https://cds.climate.copernicus.eu/datasets/reanalysis-era5-single-levels (Hersbach et al., 2020).

Author contributions

TZ and QL designed the experiments. QL and YT carried them out. QL and TZ developed the model code and performed the experiments. QL, TZ, ZC and ZH prepared the manuscript.

Competing interests

The authors declare no competing interests relevant to this study.

Acknowledgements

This paper is supported by the National Natural Science Foundation of China and the Guangdong Provincial Department of Science and Technology.

https://doi.org/10.5194/egusphere-2026-3321
Preprint. Discussion started: 19 June 2026

Financial support

This paper is supported by the National Natural Science Foundation of China (2023YFF0804900 and 52379033) and the Guangdong Provincial Department of Science and Technology (2019ZT08G090).

References

Addor, N., Newman, A. J., Mizukami, N., and Clark, M. P.: The CAMELS data set: catchment attributes and meteorology for large-sample studies, Hydrol. Earth Syst. Sci., 21, 5293–5313, https://doi.org/10.5194/hess-21-5293-2017, 2017.

Alfieri, L., Lorini, V., Hirpa, F. A., Harrigan, S., Zsoter, E., Prudhomme, C., and Salamon, P.: A global streamflow reanalysis for 1980–2018, J HYDROL X, 6, 100049, https://doi.org/10.1016/j.hydroa.2019.100049, 2020.

Anderson, B. J., Slater, L. J., Dadson, S. J., Blum, A. G., and Prosdocimi, I.: Statistical Attribution of the Influence of Urban and Tree Cover Change on Streamflow: A Comparison of Large Sample Statistical Approaches, Water Resour. Res., 58, e2021WR030742, https://doi.org/10.1029/2021WR030742, 2022.

Anderson, B. J., Slater, L. J., Rapson, J., Brunner, M. I., Dadson, S. J., Yin, J., and Buechel, M.: Stationarity Assumptions in Streamflow Sensitivity to Precipitation May Bias Future Projections, Earth's Future, 13, e2025EF006188, https://doi.org/10.1029/2025EF006188, 2025.

Chen, Z., Zhao, T., Tu, T., Tu, X., and Chen, X.: PairwiseIHA: A python toolkit to detect flow regime alterations for headwater rivers, ENVIRON MODELL SOFTW, 154, 105427, https://doi.org/10.1016/j.envsoft.2022.105427, 2022.

Ficchì, A. and Stephens, L.: Climate Variability Alters Flood Timing Across Africa, GEOPHYS RES LETT, 46, 8809–8819, https://doi.org/10.1029/2019GL081988, 2019.

Frame, J. M., Kratzert, F., Gupta, H. V., Ullrich, P., and Nearing, G. S.: On strictly enforced mass conservation constraints for modelling the rainfall-runoff process, Hydrol. Process., 37, e14847, https://doi.org/10.1002/hyp.14847, 2023.

Grimaldi, S., Salamon, P., Russo, C., Disperati, J., Zsoster, E., Wiart, C. C. D., Mazzetti, C., Choulga, M., Moschini, F., Harrigan, S., Gomes, G., Jesus, C.-R., Ramos, A., Barnard, C., Hansford, E., and Prudhomme, C.: GloFAS v4.0: towards hyper-resolution hydrological modelling at global scale, EGU General Assembly 2023, Vienna, Austria, EGU23-3410, https://doi.org/10.5194/egusphere-egu23-3410, 2023.

Harrigan, S., Zsoter, E., Alfieri, L., Prudhomme, C., Salamon, P., Wetterhall, F., Barnard, C., Cloke, H., and Pappenberger, F.: GloFAS-ERA5 operational global river discharge reanalysis 1979–present, Earth Syst. Sci. Data, 12, 2043–2060, https://doi.org/10.5194/essd-12-2043-2020, 2020.

Harrigan, S., Zsoter, E., Cloke, H., Salamon, P., and Prudhomme, C.: Daily ensemble river discharge reforecasts and real-time forecasts from the operational Global Flood Awareness System, HYDROL EARTH SYST SC, 27, 1–19, https://doi.org/10.5194/hess-27-1-2023, 2023.

Hersbach, H., Bell, B., Berrisford, P., Hirahara, S., Horányi, A., Muñoz-Sabater, J., Nicolas, J., Peubey, C., Radu, R., Schepers, D., Simmons, A., Soci, C., Abdalla, S., Abellan, X., Balsamo, G., Bechtold, P., Biavati, G., Bidlot, J., Bonavita, M., De Chiara, G., Dahlgren, P., Dee, D., Diamantakis, M., Dragani, R., Flemming, J., Forbes, R., Fuentes, M., Geer, A., Haimberger, L.,

https://doi.org/10.5194/egusphere-2026-3321
Preprint. Discussion started: 19 June 2026

Healy, S., Hogan, R. J., Hólm, E., Janisková, M., Keeley, S., Laloyaux, P., Lopez, P., Lupu, C., Radnoti, G., de Rosnay, P., Rozum, I., Vamborg, F., Villaume, S., and Thépaut, J.: The ERA5 global reanalysis, Quart J Royal Meteoro Soc, 146, 1999–2049, https://doi.org/10.1002/qj.3803, 2020.

Huang, Z. and Zhao, T.: Predictive performance of ensemble hydroclimatic forecasts: Verification metrics, diagnostic plots and forecast attributes, WIRES WATER, 9, e1580, https://doi.org/10.1002/wat2.1580, 2022.

Ishida, K., Ercan, A., Nagasato, T., Kiyama, M., and Amagasaki, M.: Use of one-dimensional CNN for input data size reduction in LSTM for improved computational efficiency and accuracy in hourly rainfall-runoff modeling, J. Environ. Manage., 359, 120931, https://doi.org/10.1016/j.jenvman.2024.120931, 2024.

Liu, L. and Lei, H.: Advanced stepwise machine learning integration of near-real-time precipitation products in China's flood-prone basins, ATMOS RES, 327, 108197, https://doi.org/10.1016/j.atmosres.2025.108197, 2026.

Liu, L., Zhou, L., Gusyev, M., and Ren, Y.: Unravelling and improving the potential of global discharge reanalysis dataset in streamflow estimation in ungauged basins, J CLEAN PROD, 419, 138282, https://doi.org/10.1016/j.jclepro.2023.138282, 2023.

Ma, X., Ma, Y., Ju, Q., Liu, C., Jin, J., Xiao, Y., Liu, H., and Wang, G.: A spatiotemporally differentiated hybrid hydrological modeling strategy with dynamically adaptive runoff generation modes, J HYDROL, 673, 135480, https://doi.org/10.1016/j.jhydrol.2026.135480, 2026.

Mbuvha, R., Adounkpe, J. Y. P., Mongwe, W. T., Houngnibo, M., Newlands, N., and Marwala, T.: Imputation of Missing Streamflow Data at Multiple Gauging Stations in Benin Republic, https://arxiv.org/abs/2211.11576v1, 17 November 2022.

McMillan, H.: Linking hydrologic signatures to hydrologic processes: A review, Hydrological Processes, 34, 1393–1409, https://doi.org/10.1002/hyp.13632, 2020.

Meng, H. and Zhao, T.: Evaluation of the hydrological utility of the GPM IMERG satellite precipitation products, Atmos. Res., 322, 108139, https://doi.org/10.1016/j.atmosres.2025.108139, 2025.

Miao, C., Gou, J., Hu, J., and Duan, Q.: Impacts of Different Satellite-Based Precipitation Signature Errors on Hydrological Modeling Performance Across China, Earth's Future, 12, e2024EF004954, https://doi.org/10.1029/2024EF004954, 2024.

Nanding, N., Wu, H., Tao, J., Maggioni, V., Beck, H. E., Zhou, N., Huang, M., and Huang, Z.: Assessment of Precipitation Error Propagation in Discharge Simulations over the Contiguous United States, J HYDROMETEOROL, 22, 1987–2008, https://doi.org/10.1175/JHM-D-20-0213.1, 2021a.

Nanding, N., Rico-Ramirez, M. A., Han, D., Wu, H., Dai, Q., and Zhang, J.: Uncertainty assessment of radar-raingauge merged rainfall estimates in river discharge simulations, J HYDROL, 603, 127093, https://doi.org/10.1016/j.jhydrol.2021.127093, 2021b.

Nearing, G., Cohen, D., Dube, V., Gauch, M., Gilon, O., Harrigan, S., Hassidim, A., Klotz, D., Kratzert, F., Metzger, A., Nevo, S., Pappenberger, F., Prudhomme, C., Shalev, G., Shenzis, S., Tekalign, T. Y., Weitzner, D., and Matias, Y.: Global prediction of extreme floods in ungauged watersheds, Nature, 627, 559–563, https://doi.org/10.1038/s41586-024-07145-1, 2024.

Newman, A. J., Clark, M. P., Sampson, K., Wood, A., Hay, L. E., Bock, A., Viger, R. J., Blodgett, D., Brekke, L., Arnold, J. R., Hopson, T., and Duan, Q.: Development of a large-sample watershed-scale hydrometeorological data set for the contiguous USA: data set characteristics and assessment of regional variability in hydrologic model performance, Hydrol. Earth Syst. Sci., 19, 209–223, https://doi.org/10.5194/hess-19-209-2015, 2015.

https://doi.org/10.5194/egusphere-2026-3321
Preprint. Discussion started: 19 June 2026

Nourani, V., Kheirieh, S., Kantoush, S. A., and Huang, J. J.: Bias correction of Global Flood Awareness System (GloFAS) data for multi-station river flow prediction by ensemble modelling, ENG APPL COMP FLUID, 20, 2665857, https://doi.org/10.1080/19942060.2026.2665857, 2026.

Over, T., Marti, M., Ortiz, J., and Podzorski, H.: The joint effect of changes in urbanization and climate on trends in floods: A comparison of panel and single-station quantile regression approaches, J. Hydrol., 648, 132281, https://doi.org/10.1016/j.jhydrol.2024.132281, 2025.

Prudhomme, C., Zsótér, E., Matthews, G., Melet, A., Grimaldi, S., Zuo, H., Hansford, E., Harrigan, S., Mazzetti, C., de Boisseson, E., Salamon, P., and Garric, G.: Global hydrological reanalyses: The value of river discharge information for world-wide downstream applications – The example of the Global Flood Awareness System GloFAS, METEOROL APPL, 31, e2192, https://doi.org/10.1002/met.2192, 2024.

Rahman, Md. H., Zaman, I. U., Ahmed, K., Bushra, F., Khan, N. Z., and Rahman, R. M.: Machine Learning Techniques for River Discharge Prediction Using ERA5 and GloFAS Data, in: 2022 IEEE 13th Annual Ubiquitous Computing, Electronics & Mobile Communication Conference (UEMCON), 2022 IEEE 13th Annual Ubiquitous Computing, Electronics & Mobile Communication Conference (UEMCON), 0554–0560, https://doi.org/10.1109/UEMCON54665.2022.9965629, 2022.

Senent-Aparicio, J., Blanco-Gómez, P., López-Ballesteros, A., Jimeno-Sáez, P., and Pérez-Sánchez, J.: Evaluating the Potential of GloFAS-ERA5 River Discharge Reanalysis Data for Calibrating the SWAT Model in the Grande San Miguel River Basin (El Salvador), REMOTE SENS-BASEL, 13, 3299, https://doi.org/10.3390/rs13163299, 2021.

Steinschneider, S., Yang, Y.-C. E., and Brown, C.: Panel regression techniques for identifying impacts of anthropogenic landscape change on hydrologic response, Water Resour. Res., 49, 7874–7886, https://doi.org/10.1002/2013WR013818, 2013.

Tang, G., Clark, M. P., Knoben, W. J. M., Liu, H., Gharari, S., Arnal, L., Beck, H. E., Wood, A. W., Newman, A. J., and Papalexiou, S. M.: The Impact of Meteorological Forcing Uncertainty on Hydrological Modeling: A Global Analysis of Cryosphere Basins, WATER RESOUR RES, 59, e2022WR033767, https://doi.org/10.1029/2022WR033767, 2023.

Thornton, M. M., Thornton, P. E., Wei, Y., Mayer, B. W., Cook, R. B., and Vose, R. S.: Daymet: monthly climate summaries on a 1-km grid for North America, Version 3. ORNL DAAC, Oak Ridge, Tennessee, USA, 2016.

Wang, J., Chen, X., Liu, J., and Hu, Q.: Changes of Precipitation-Runoff Relationship Induced by Climate Variation in a Large Glaciated Basin of the Tibetan Plateau, Journal of Geophysical Research: Atmospheres, 126, e2020JD034367, https://doi.org/10.1029/2020JD034367, 2021.

Wang, J., Zhuo, L., Han, D., Liu, Y., and Rico-Ramirez, M. A.: Hydrological Model Adaptability to Rainfall Inputs of Varied Quality, Water Resour. Res., 59, e2022WR032484, https://doi.org/10.1029/2022WR032484, 2023.

Wang, N., Sun, F., Liu, W., Yang, S., Wang, H., Feng, Y., and Huang, Q.: Climate drives observational changes in hydrological extremes across most global regions, INNOVATION-AMSTERDAM, 7, 101171, https://doi.org/10.1016/j.xinn.2025.101171, 2026.

Wu, H., Adler, R. F., Tian, Y., Gu, G., and Huffman, G. J.: Evaluation of Quantitative Precipitation Estimations through Hydrological Modeling in IFloodS River Basins, J HYDROMETEOROL, 18, 529–553, https://doi.org/10.1175/JHM-D-15-0149.1, 2017.

Yang, Y., Pan, M., Lin, P., Beck, H. E., Zeng, Z., Yamazaki, D., David, C. H., Lu, H., Yang, K., Hong, Y., and Wood, E. F.: Global Reach-Level 3-Hourly River Flood Reanalysis (1980–2019), B AM METEOROL SOC, 102, E2086–E2105, https://doi.org/10.1175/BAMS-D-20-0057.1, 2021.

https://doi.org/10.5194/egusphere-2026-3321
Preprint. Discussion started: 19 June 2026

Zhang, J., Wang, Y., Zhao, L., Sun, R., Sun, J., Wang, S., Xu, S., and Yang, Z.: Identification of key factors influencing monthly runoff simulation through the integration of deep learning and physically-based hydrological models, Environ. Modell. Softw., 199, 106927, https://doi.org/10.1016/j.envsoft.2026.106927, 2026.

Zhao, T., Chen, Z., Tu, T., Yan, D., and Chen, X.: Unravelling the potential of global streamflow reanalysis in characterizing local flow regime, SCI TOTAL ENVIRON, 838, 156125, https://doi.org/10.1016/j.scitotenv.2022.156125, 2022.

Zhao, T., Chen, Z., Tian, Y., Zhang, B., Li, Y., and Chen, X.: A decomposition approach to evaluating the local performance of global streamflow reanalysis, HYDROL EARTH SYST SC, 28, 3597–3611, https://doi.org/10.5194/hess-28-3597-2024, 2024.

Zhu, Y., Sang, Y.-F., Wang, B., Lutz, A., Hu, S., Chen, D., and Singh, V. P.: Heterogeneity in Spatiotemporal Variability of High Mountain Asia's Runoff and Its Underlying Mechanisms, WATER RESOUR RES, 59, e2022WR032721, https://doi.org/10.1029/2022WR032721, 2023.